



Probing the interaction of midazolam with human serum albumin: a biophysical investigation

Xingang Ma¹ · Yulin Zhu² · Kun Xie³

Received: 6 March 2020 / Accepted: 24 July 2020 / Published online: 17 September 2020
© Springer Nature B.V. 2020

Abstract

Herein, the spectroscopic methods were applied for investigating the interaction between human serum albumin (HSA) and midazolam in simulated physiological environments. The fluorescence quenching of HSA by midazolam followed the static mode. The association constant at 293 K was obtained as $1.73 \times 10^4 \text{ M}^{-1}$ with probably one binding site between midazolam and HSA. The results of thermodynamic parameters revealed that the hydrogen bonding was the dominating force in the interaction. The results of UV–Vis spectra, synchronous fluorescence, and circular dichroism results showed that binding with midazolam subtly changed the HSA's conformation along with the secondary structure. The results of Förster resonance energy transfer showed a possible 3.48 nm energy transfer distance with Trp-214 to midazolam. This study aimed to provide valuable information for further research on pharmacological mechanisms and the toxicological and distribution of midazolam in vivo.

Keywords Human serum albumin · Midazolam · Interaction mechanism · Spectroscopy

Introduction

Taking about 50% to 60% percent of the plasma protein amount, HSA (Fig. 1a) is the main component of soluble protein in the human circulatory system [1, 2]. The critical function of this kind of protein is that it could act as a transporter for amine-terminated dendrimers, fatty acids, drugs, and other compounds [3]. The first process in the complicated mechanism of its biological action was the binding and molecular recognition of drugs by the target proteins. It is expected that the details about the biological processes' energetic and structural properties could provide

a fundamental understanding of the toxicological action with a rational basis.

Midazolam (Fig. 1b) is a type of drugs called benzodiazepines, and it is a short-acting hypnotic-sedative drug used for an anxiolytic anticonvulsant, muscle relaxant, amnesic properties, hypnotic and sedative [4]. This drug is outstanding among this class of drugs due to its rapid action and short duration of action. Midazolam can be used by intramuscular, rectal, intravenous routes, oral and intranasal. At present, midazolam has been widely used in diversified biomedical applications; for example, midazolam could be used as pre-anesthetic medication and adjunct to local anesthesia in endoscopic procedures, cardiac surgery, and dentistry. However, when administrated into veins, midazolam could bind with serum albumin in blood before it targets the receptor [5]. Thus, studying the interaction of midazolam and HSA would make an essential contribution to related toxicological and pharmacological research. Although Khan and Tang have investigated the interaction of midazolam and human serum albumin, the binding induced conformational changes were not fully addressed, and discrepancy in synchronous spectroscopy led to different conclusions [6, 7].

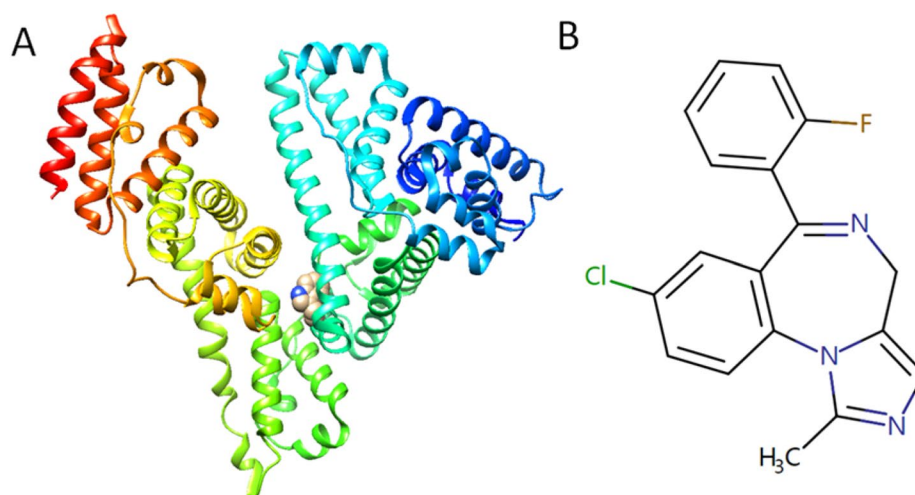
This study aimed to use fluorescence and UV–Vis spectroscopy to investigate the association between midazolam and HSA. Besides, CD spectroscopy was also used to

Electronic supplementary material The online version of this article (<https://doi.org/10.1007/s10847-020-01016-8>) contains supplementary material, which is available to authorized users.

✉ Kun Xie
2277316289@qq.com

- ¹ Department of Anesthesiology, Zibo Maternal and Child Health Hospital, Zibo 255000, China
- ² Department of Anesthesiology, Yantai Hospital, Yantai 264000, China
- ³ Department of Anesthesiology, The Second Hospital, Cheeloo College of Medicine, Shandong University, Jinan 250033, China

Fig. 1 **a** Structure of HSA with Trp-214 residue indicated. **b** Molecular structure of the midazolam molecule



understand the role of serum albumin act as a carrier for midazolam under the physiological conditions. We obtained the thermodynamic parameters and quenching constants at different temperatures. This study provided the binding mechanism between midazolam with HSA.

Materials and methods

Materials

Both phosphate buffer powder and fatty-acid-free HSA were procured from Sigma, USA, whereas midazolam (purity more than 99%) was procured from the Tokyo Chemical Industry (Tokyo, Japan). Deionized water was used throughout our study. The preparation of the stock solution was to dissolve 1×10^{-5} M HSA in a 0.2 M phosphate buffer solution. Other chemicals employed in this study were bought from Sinopharm (Beijing, China).

Methods

The Hitachi 7500 fluorophotometer was used for the measurements of fluorescence with a temperature accuracy of 0.1 K. The measuring range of the emission spectrum was set from 280 to 420 nm, and the intrinsic fluorescence was measured by exciting HSA at 278 nm. By setting the wavelength difference at 15 nm and 60 nm, synchronous fluorescence was conducted, and the spectra were recorded within a range of 250–330 nm. A special fluorescent cuvette with four translucent quartz sides and 1 cm path length was used.

The FLS920 spectrophotometer (Edinburg, England) was used to measure the fluorescence lifetimes of HSA in the presence of different concentrations of midazolam ($\lambda_{\text{ex}} = 278$ nm, $\lambda_{\text{em}} = 340$ nm).

The measurement of CD spectra was conducted by a Jasco-815 (Jasco, Tokyo, Japan). In the presence of different concentrations of midazolam, the protein CD spectra were obtained by a 1 cm path length cuvette and the wavelength was set from 190 to 240 nm. The CD spectra were calculated according to the CDpro software package.

The Shimadzu UV2550 spectrophotometer (Shimadzu, Tokyo, Japan) was used for analyzing the absorbance spectra of HSA in a phosphate buffer solution with different concentrations of the drug. A 2 nm slit width and a scanning speed of 50 nm/min had been set. The HSA concentration for each run was fixed at 1×10^{-6} M, and the concentrations of drugs were 0 and 8×10^{-5} M.

Results and discussion

HSA–midazolam interaction mechanism by fluorescence spectroscopy

Fluorescence quenching is a reduction in the quantum yield of fluorescence from a chromophore, which is caused by all kinds of molecular interactions, e.g., energy transfer, collisional quenching, and formation of a steady complex. According to the diverse mechanisms, fluorescence quenching is classifiable into two types, that is, static quenching and dynamic quenching [8, 9]. Static quenching is the result of the ground-state complex formation, while the dynamic quenching is the result of diffusion. Generally, static and dynamic quenching can be distinguished by their different temperature dependence [10, 11]. It is well-known that larger diffusion coefficients are the result of higher temperatures; thus, it is expected that dynamic quenching constants would be enhanced with the increase of temperature. On the other side, with the increasing temperature, the complexes'

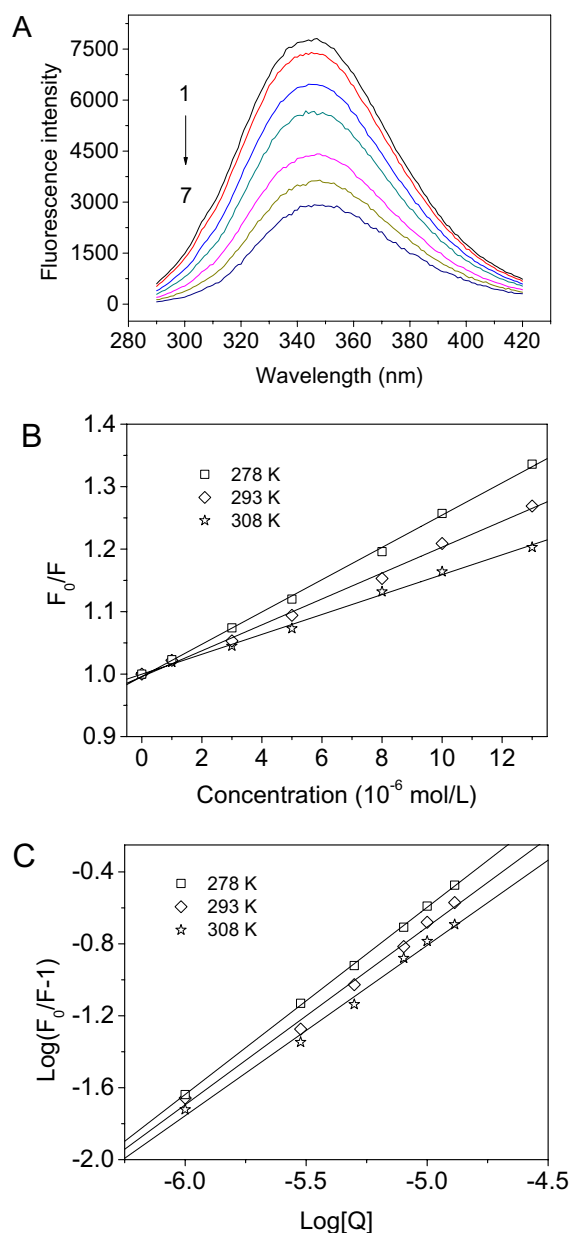


Fig. 2 a Changes in the fluorescence spectra of HSA through their titration with midazolam at 298 K. The concentration HSA is 1×10^{-6} M, and midazolam concentrations are 0, 1, 3, 5, 8, 10 and 13×10^{-6} M from 1 to 7. Stern–Volmer (b) and Hill (c) plots at different temperatures

Table 1 Stern–Volmer quenching constants, binding parameters, and thermodynamic parameters of HSA–midazolam system at different temperatures

T (K)	Stern–Volmer quenching constants			Binding parameters			Thermodynamic parameters		
	K_q ($M^{-1} s^{-1}$)	K_{SV} (M^{-1})	Pearson's r	K_A (M^{-1})	n	Pearson's r	ΔG ($J \cdot mol^{-1}$)	ΔS ($J \cdot mol^{-1} \cdot K^{-1}$)	ΔH ($J \cdot mol^{-1}$)
278	2.58×10^{12}	2.58×10^4	0.9994	4.05×10^4	1.04	0.9998	-2.45×10^4	37.6	
293	2.07×10^{12}	2.07×10^4	0.9981	1.73×10^4	0.99	0.9964	-2.38×10^4	37.4	-1.72×10^4
308	1.59×10^{12}	1.59×10^4	0.9999	8.51×10^3	0.95	0.9961	-2.32×10^4	24.0	

stability would decrease, and thus, the static quenching constants would be lower [12–14].

In the presence of midazolam with diverse concentrations at 293 K, the emission spectra of HSA was obtained and shown in Fig. 2a. Strong fluorescence emission of HSA with peaks at 340 nm was shown when it was excited at 278 nm. The HSA fluorescence intensity was regularly reduced when a fixed concentration of HSA was treated with various midazolam amount. Furthermore, when the midazolam solution was added, a slight red shift (345 nm to 348 nm) of the emission peak maxima was found, which revealed that when the midazolam was added, the protein chromophore was located in a more hydrophobic condition [15, 16]. Figure 2b shows the Stern–Volmer plots at 308 K, 293 K, and 278 K. It is demonstrated that the plot exhibited significant linear relationship within the investigated concentrations range in this study, and the parameters at each temperature was obtained by the Stern–Volmer formula [17–20]:

$$F_0/F = 1 + K_q \tau_0 [Q] = 1 + K_{SV} [Q]$$

where F_0 represents the fluorescence intensity without the addition of midazolam, while F represents the fluorescence intensity with the addition of midazolam. $[Q]$ represents the quencher concentration. K_{SV} is the quenching constant of the Stern–Volmer equation. K_q represents the quenching rate constant of the biological macromolecule and could be calculated by the equation: $K_q = K_{SV}/\tau_0$, where τ_0 represents the mean lifetime of the native biomolecules, the fluorescence of which is 10^{-8} s according to the literature. The values of K_q and K_{SV} at different temperatures were calculated and displayed in Table 1. During the process of dynamic interaction, the maximum quenching constant is $2.0 \times 10^{10} L mol^{-1} s^{-1}$. The results revealed that K_q value and K_{SV} value displayed a decreasing trend with the increasing temperatures. Additionally, K_q value was higher than $2.0 \times 10^{10} L mol^{-1} s^{-1}$, and this result indicated that the formation of the midazolam–HSA complex was the result of static interaction rather than dynamic collision.

In general, by the method of fluorescence lifetime measurement, static and dynamic quenching could be distinguished effectively. The time-resolved fluorescence of HSA was taken with an excitation wavelength of 278 nm. Our

results fit the sum of a single exponential decay well with a χ^2 value close to 1. As it was shown in Fig. 3, the decay profiles of HSA (from $\tau = 5.26$ ns, $\chi^2 = 1.012$ to $\tau = 5.30$ ns, $\chi^2 = 1.023$) in the presence and absence of midazolam makes no difference. Dynamic quenching is supposed to result in a variable lifetime. With the increasing amounts of quencher (midazolam), the lifetime showed an invariance, which could be ascribed to static quenching other than a dynamic one. Both the theoretical results and experimental results in this study simultaneously suggested the formation of a ground-state complex.

The binding constant of to HSA and value of midazolam molecules bound per protein (n) can be obtained by using the Hill equation to measure the static quenching [21]:

$$\lg \frac{F_0 - F}{F} = \lg K_A + n \lg [Q]$$

Accordingly, the plot of $\log [(F_0 - F)/F]$ vs. $\log [Q]$ was displayed in Fig. 2c. The related parameters were calculated and represented in Table 1. The n value for the HSA–midazolam complex was 1 according to the slope, which suggested that one protein molecule was bound by one midazolam molecule at 297 K. The binding constants K_A acquired at 297 K was $4.49 \times 10^4 \text{ M}^{-1}$. Compared with other complexes, which are strong ligand–protein, the results of the association constants of the HSA–midazolam system suggested low binding affinity [11, 22, 23].

The acting forces between HSA and drugs were expressed by the thermodynamic parameters relying on temperatures. There are some dominated interaction forces between biomolecules and drugs, such as van der Waals or H-bonding interactions, hydrophobic interactions, and electrostatic interactions. The interaction forces of HSA with midazolam were illustrated by the thermodynamic parameters, such as entropy changes (ΔS°), enthalpy changes (ΔH°), and free energy changes (ΔG°) of the interactions. If there is no significant change of enthalpy (ΔH°) occurred in the range of

temperature, the value of ΔS° and ΔH° can be measured by van't Hoff equation [1]:

$$\ln \left(\frac{K_2}{K_1} \right) = \frac{\Delta H^\circ}{R} \left(\frac{1}{T_1} - \frac{1}{T_2} \right)$$

where R represents the gas constant, and K represents the binding constants at different temperatures. The value of enthalpy change (ΔH°) was determined by the slope of the plot (Fig. 4). And the free energy change (ΔG°) was calculated by the equations below:

$$\Delta G^\circ = \Delta H^\circ - T\Delta S^\circ = -RT \ln K^\circ$$

The ΔH° , ΔG° , and ΔS° values were shown in Table 1. The negative value of free energy (ΔG°) suggested the spontaneous binding process. The positive value of ΔS° and negative value of ΔH° demonstrated that this process is enthalpy-driven as a result of $T\Delta S^\circ < \Delta H^\circ$. The enthalpy value was $-1.72 \times 10^4 \text{ J mol}^{-1}$, which corresponds to the formation of a hydrogen bond in HSA–midazolam complex.

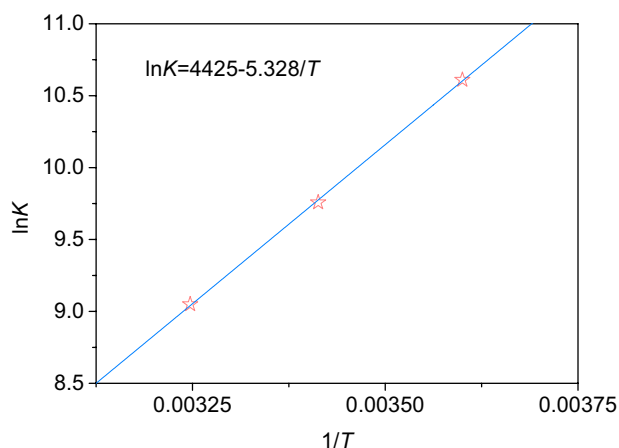


Fig. 4 van't Hoff plot of the HSA–midazolam system

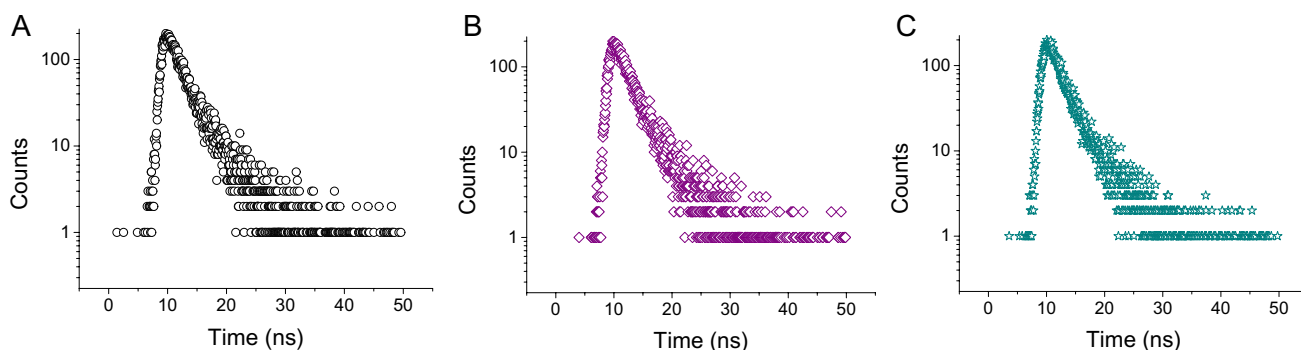


Fig. 3 Time-resolved fluorescence decay profile of HSA–midazolam. The concentration HSA is $1 \times 10^{-6} \text{ M}$, and midazolam concentration is 0 (a), 5 (b), and 10 (c) $\times 10^{-6} \text{ M}$

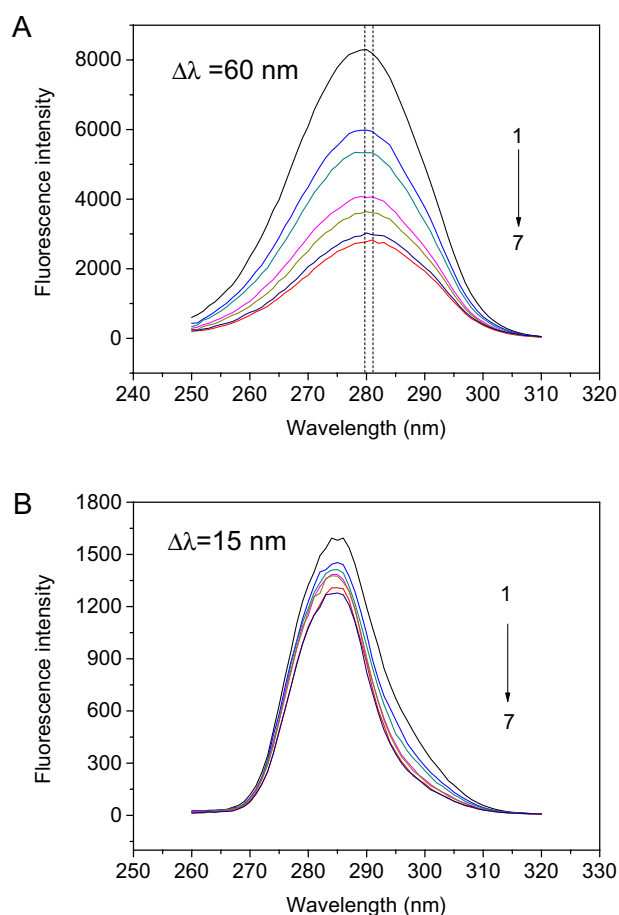


Fig. 5 Synchronous fluorescence spectra of tryptophan (a $\Delta\lambda = 15$ nm) and tyrosine (b $\Delta\lambda = 60$ nm)

Synchronous fluorescence spectroscopy study

Since the synchronous fluorescence spectroscopic technique was discovered by Lloyd and Evett in the 1970s, this technique has been applied for understanding the molecular environment in the vicinity of the low-concentration fluorophore molecules under physiological conditions. By setting $\Delta\lambda$ at 15 nm, the results of synchronous fluorescence spectrum suggested the spectral property of Tyr residues, while when $\Delta\lambda$ is 60 nm, the result suggested the property of Trp residues (Supplementary Data Fig. S1) [24]. The maximum emission wavelengths of Tyr residue and Trp residue in the protein molecule are associated with the polarity of the environment; the changes of protein conformation can be reflected by the fluctuation of the maximum emission wavelengths. Figure 5 displayed the effect of midazolam on HSA. According to Fig. 5a, we found a slight red shift (from 279.5 to 281.5 nm) of maximum emission wavelength at the study range of midazolam concentration when $\Delta\lambda$ was 60 nm. However, as was shown in Fig. 5b, the maximum emission wavelength remains unchanged at the study range of midazolam concentration when $\Delta\lambda$ was 15 nm. Red shift of the maximum emission wavelength suggested that the HSA conformation has been changed and the hydrophobicity around the Trp residues was decreased, whereas the polarity was increased. However, during the binding process, no changes in microenvironment were found around the Tyr residues.

3D fluorescence spectra of the protein–drug complex

The 3D fluorescence spectra could give all the information on fluorescence characteristics, and the spectra of

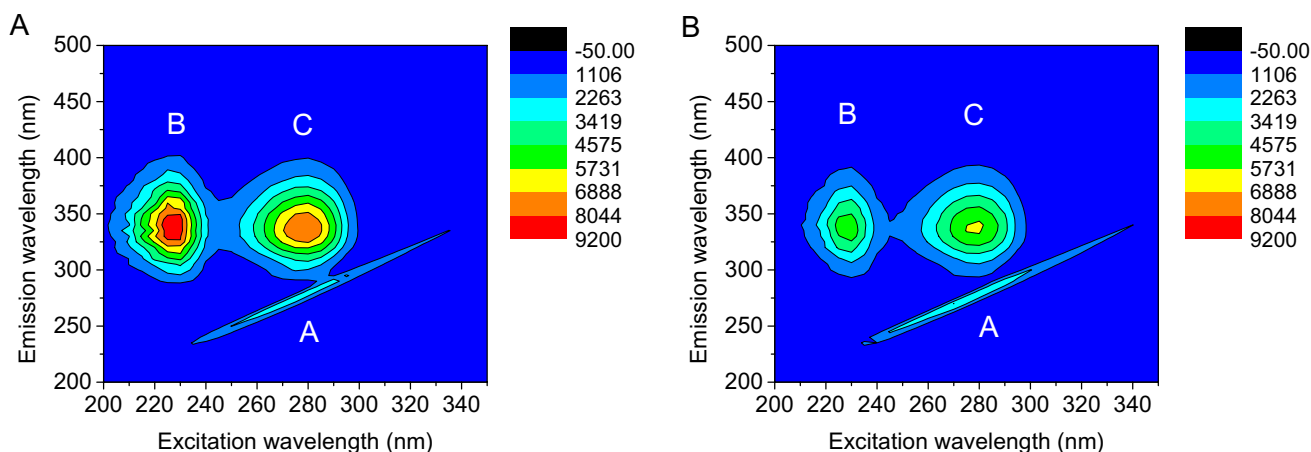
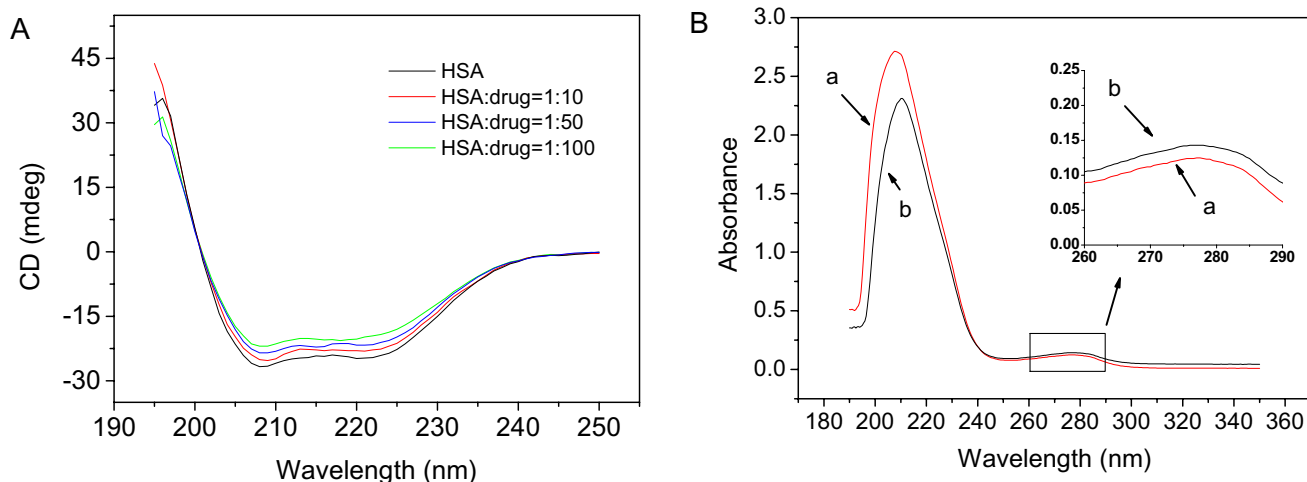


Fig. 6 Three-dimensional fluorescence spectra of HSA–midazolam. The concentration HSA is 1×10^{-6} M, and midazolam concentration is 0 (a) and 5 (b) $\times 10^{-6}$ M

Table 2 Three-dimensional fluorescence spectral characteristics of the HSA and HSA–midazolam systems

Peaks	HSA			HSA–midazolam		
	Peak position $\lambda_{\text{ex}}/\lambda_{\text{em}}$ (nm/nm)	Stokes $\Delta\lambda$ (nm)	Fluorescence intensity	Peak position $\lambda_{\text{ex}}/\lambda_{\text{em}}$ (nm/nm)	Stokes $\Delta\lambda$ (nm)	Fluorescence intensity
B	278/337	59	7560	278/337	59	5934
C	225/337	112	8721	225/338	113	5635

**Fig. 7** a CD spectra of HSA (2×10^{-7} M) in the presence of midazolam. Concentrations of the midazolam are 0, 2, 10, and 20×10^{-6} M. b UV–Vis of HSA (1×10^{-6} M) in the presence of midazolam. Concentrations of midazolam are 0, and 10×10^{-6} M

midazolam–HSA complex and HSA were displayed in Fig. 6, with the related parameters displayed in Table 2. The conformation alteration and microenvironment of HSA were investigated by comparing the alteration of HSA in the presence and absence of midazolam. According to Fig. 6, peak A represents the Rayleigh scattering peak (the excitation wavelengths are equal to the emission wavelengths), and peak B represents the spectral characteristic of fluorophores of HSA, whereas peak C reveals the polypeptide backbone structural behavior of HSA. It is observed that the peak A fluorescence intensity increased when the adding of midazolam. The reason for this result could be ascribed to the HSA–midazolam complex formation, which increased the protein in volume and caused the scattering effect enhanced. When midazolam was added in HSA, the decrease in fluorescence intensities of peaks B and peaks C was observed; meanwhile, a red-shifted peak C was also found (from 337 to 338 nm). The result suggested that the midazolam–HSA interaction could make the polypeptide backbone of HSA slightly unfold, and midazolam was located around the Trp residue.

CD and UV–Vis spectroscopy to study the conformation of HSA

The CD spectra of HSA with midazolam in buffer were displayed in Fig. 7a. The two negative bands of HSA at 222 nm

Table 3 Secondary structure alterations of HSA induced by midazolam in accordance with Fig. 7a

Sample	Structural elements			
	α -helix ($\pm 3\%$)	β -sheet ($\pm 1\%$)	β -turn ($\pm 1\%$)	Random coil ($\pm 3\%$)
1	55.7	10.8	7.2	26.7
2	54.2	11.2	7.4	27.2
3	51.9	12.5	8.5	27.1
4	48.9	13.5	7.5	30.1

and 208 nm were illustrated, which suggested the typical α -helix structure of the protein [25]. When treated with midazolam, the intensity of HSA bands regularly decreased, suggesting that the binding with midazolam could affect the protein's secondary structure, especially the α -helix structure. The CDpro software package was used to calculate the secondary structural contents, and the results were displayed in Table 3. The decrement of α -helical content (55.7–54.2–51.9–48.9%) along with the β -sheet content increase (10.8–11.2–12.5–13.5%) suggested that midazolam destroyed the raw HSA conformation. The binding of midazolam to HSA destroyed the networks of hydrogen-bonding

within the protein. For HSA, the skeleton of the polypeptide was getting tender, and the conformation of biomolecule would be altered easily.

As a sensitive technique, UV–Vis spectroscopy was widely applied in exploring the structural alteration of the protein [26, 27]. The UV–Vis absorption spectra of HSA influenced by drugs were shown in Fig. 7b. According to Fig. 7b a strong absorption peak, and a shoulder peak were observed at the wavelength of 210 nm and 278 nm, which are assigned to the HSA backbone structure and the adsorption of the amino acid residues (Tyr, Trp, and Phe), respectively [28, 29]. It was found that the spectra of HSA-drug differed from HSA, especially in the range of 200 nm to 220 nm. Changes around 210 nm of the spectrum suggested that characteristic polypeptide backbone structure of HSA was destroyed upon interacting with midazolam. At the same time, the change of absorbance at around 278 nm showed different tendencies with that at 210 nm, suggested that midazolam could cause variation of the microenvironment of amino acid residues. All these results were in agreement with the synchronous, steady/time-resolved, and 3D fluorescence data.

Energy transfer from HSA to midazolam

Förster resonance energy transfer (FRET) is a powerful technique for determining the spatial distance of the two points in proteins (between an acceptor and a donor) [30]. Meanwhile, distances of FRET between the two points were widely used to understand the protein–protein interactions, protein folding pathways, monomer–dimer equilibrium, and conformational changes upon ligand binding.

Based on Förster's theory, the energy transfer efficiency (E) from Trp214 residue in HSA to midazolam was associated with the distance (r) between the donor and the acceptor by the following formula:

$$E = 1 - \frac{F}{F_0} = \frac{R_0^6}{R_0^6 + r^6}$$

where R_0 represents the critical distance of acceptor and donor when the transfer efficiency is 50%, and it can be determined as follows:

$$R_0^6 = 8.8 \times 10^{-25} k^2 N^{-4} \Phi J$$

where N represents the medium refractive index; k^2 represents the spatial orientation factor of the dipole, which is equal to 2/3; Φ represents the fluorescence quantum yield of the donor; and J represents the integral area of the fluorescence spectrum of the donor to the UV–Vis spectrum of the acceptor (Fig. S2), which is determined by following [13]:

$$J = \frac{\sum F(\lambda)\epsilon(\lambda)\lambda^4\Delta\lambda}{\sum F(\lambda)\Delta\lambda}$$

where $F(\lambda)$ represents the donor's fluorescence intensity at a wavelength of λ while $\epsilon(\lambda)$ represents the molar absorption coefficient of the acceptor at the corresponding wavelength. For HSA–ligand bindings, it was reported that $\Phi=0.15$ and $N=1.336$ [30]. Thus based on the equations above, the calculations were that $r=3.97$ nm, $R_0=4.27$ nm, $E=0.117$, and $J=4.84 \times 10^{-15} \text{ cm}^3 \text{ M}^{-1}$ for midazolam–HSA binding. Meanwhile, the distance between Trp214 residue and midazolam was below 8 nm, which is in line with Förster energy transfer.

Conclusions

In this study, the HSA–midazolam interaction has been revealed by various spectroscopic assays. The results demonstrated a moderate affinity of midazolam binding to HSA, and a static quenching mechanism could be obtained in this process. The quenching and binding constants were determined with the Stern–Volmer and Hill equations, respectively. Meanwhile, the thermodynamic constants, including the negative value of ΔS° , ΔG° , and ΔH° indicate that van der Waals and H-bonding were the dominating force in the interaction. The calculated distance (r) between Trp-214 of HSA and midazolam was 3.71 nm, which is consistent with the Förster non-radioactive resonance energy-transfer theory. Furthermore, according to the results of UV–Vis, 3D fluorescence, and CD, the conformation of HSA was changed upon association with midazolam. The outcomes of this work provide fundamental information for understanding the mechanistic pathway of the midazolam pharmacokinetics.

References

1. Lu, D.W., Zhao, X.C., Zhao, Y.C., Zhang, B.C., Zhang, B., Geng, M.Y., Liu, R.T.: Binding of Sudan II and Sudan IV to bovine serum albumin: comparison studies. *Food Chem. Toxicol.* **49**(12), 3158–3164 (2011)
2. Soltanabadi, O., Atri, M.S., Bagheri, M.: Spectroscopic analysis, docking and molecular dynamics simulation of the interaction of cinnamaldehyde with human serum albumin. *J. Incl. Phenom. Macrocycl. Chem.* **91**(3–4), 189–197 (2018)
3. Meloun, B., Moravek, L., Kostka, V.: Complete amino acid sequence of human serum albumin. *FEBS Lett.* **58**(1), 134–137 (1975)
4. Reves, J.D., Fragen, R.J., Vinik, H.R., Greenblatt, D.J.: Midazolam: pharmacology and uses. *Anesthesiology* **62**(3), 310–324 (1985)
5. Allonen, H., Ziegler, G., Klotz, U.: Midazolam kinetics. *Clin. Pharmacol. Ther.* **30**(5), 653–661 (1981)

6. Khan, S.N., Islam, B., Khan, A.U.: Probing midazolam interaction with human serum albumin and its effect on structural state of protein. *Int. J. Integ. Biol* **1**, 102–112 (2007)
7. Tang, C.-R., Cao, G.-Z., Hu, L.-F., Xu, R.-A., Gao, X.-C., Zheng, Y.-M.: Interaction between midazolam and human serum albumin by fluorescence spectrum. *China. Pharmacy* **41**, 22 (2012)
8. Zhao, X., Lu, D., Liu, Q.S., Li, Y., Feng, R., Hao, F., Qu, G., Zhou, Q., Jiang, G.: Hematological effects of gold nanorods on erythrocytes: hemolysis and hemoglobin conformational and functional changes. *Adv. Sci.* **4**(12), 1700296 (2017)
9. Dorraji, M.S.S., Azar, V.P., Rasoulifard, M.H.: Interaction between deferiprone and human serum albumin: multi-spectroscopic, electrochemical and molecular docking methods. *Eur. J. Pharm. Sci.* **64**, 9–17 (2014)
10. Zhao, X.C., Liu, R.T., Chi, Z.X., Teng, Y., Qin, P.F.: New insights into the behavior of bovine serum albumin adsorbed onto carbon nanotubes: comprehensive spectroscopic studies. *J. Phys. Chem. B* **114**(16), 5625–5631 (2010)
11. Mandeville, J.S., Tajmir-Riahi, H.A.: Complexes of dendrimers with bovine serum albumin. *Biomacromol* **11**(2), 465–472 (2010)
12. Tod, M., Mir, O., Bancelin, N., Coriat, R., Thomas-Schoemann, A., Taieb, F., Boudou-Rouquette, P., Ropert, S., Michels, J., Abbas, H.: Functional and clinical evidence of the influence of sorafenib binding to albumin on sorafenib disposition in adult cancer patients. *Pharm. Res.* **28**(12), 3199–3207 (2011)
13. Punith, R., Seetharamappa, J.: Spectral characterization of the binding and conformational changes of serum albumins upon interaction with an anticancer drug, anastrozole. *Spectrochim Acta Part A* **92**, 37–41 (2012)
14. Hebia, C., Bekale, L., Chanphai, P., Agbebavi, J., Tajmir-Riahi, H.A.: Trypsin inhibitor complexes with human and bovine serum albumins: TEM and spectroscopic analysis. *J. Photochem. Photobiol. B* **130**, 254–259 (2014)
15. Zhao, X., Hao, F., Lu, D., Liu, W., Zhou, Q., Jiang, G.: Influence of the surface functional group density on the carbon-nanotube-induced α -chymotrypsin structure and activity alterations. *ACS Appl. Mater. Interfaces.* **7**(33), 18880–18890 (2015)
16. Jana, S., Dalapati, S., Ghosh, S., Guchhait, N.: Study of microheterogeneous environment of protein Human Serum Albumin by an extrinsic fluorescent reporter: a spectroscopic study in combination with Molecular Docking and Molecular Dynamics Simulation. *J. Photochem. Photobiol. B* **112**, 48–58 (2012)
17. Zhao, X., Liu, R., Teng, Y., Liu, X.: The interaction between Ag(+) and bovine serum albumin: a spectroscopic investigation. *Sci. Total Environ.* **409**(5), 892–897 (2011)
18. Kitamura, M., Murakami, K., Yamada, K., Kawai, K., Kunishima, M.: Binding of sulforhodamine B to human serum albumin: a spectroscopic study. *Dyes Pigm.* **99**(3), 588–593 (2013)
19. Zheng, Y.-R., Suntharalingam, K., Johnstone, T.C., Yoo, H., Lin, W., Brooks, J.G., Lippard, S.J.: Pt(IV) prodrugs designed to bind non-covalently to human serum albumin for drug delivery. *J. Am. Chem. Soc.* **136**(24), 8790–8798 (2014)
20. Xu, C., Zhao, X., Wang, L., Zhang, X., Wang, Y., Lan, J.: Protein conjugation with gold nanoparticles: spectroscopic and thermodynamic analysis on the conformational and activity of serum albumin. *J. Nanosci. Nanotechnol.* **18**(11), 7818–7823 (2018)
21. Xu, F., Zhang, L., He, L., Gu, W., Fang, F., Wu, Q., Zhao, B.: Molecular mechanism on the interaction between alisols and human serum albumin. *Acta Chim. Sinica* **69**(19), 2228–2234 (2011)
22. Bolli, A., Marino, M., Rimbach, G., Fanali, G., Fasano, M., Ascenzi, P.: Flavonoid binding to human serum albumin. *Biochem. Biophys. Res. Commun.* **398**(3), 444–449 (2010)
23. Hussein, B.H.M.: Spectroscopic studies of 7, 8-dihydroxy-4-methylcoumarin and its interaction with bovine serum albumin. *J. Lumin.* **131**(5), 900–908 (2011)
24. Gokara, M., Sudhamalla, B., Amooru, D.G., Subramanyam, R.: Molecular interaction studies of trimethoxy flavone with human serum albumin. *PLoS ONE* **5**(1), e8834 (2010)
25. Zhao, X., Sheng, F., Zheng, J., Liu, R.: Composition and stability of anthocyanins from purple solanum tuberosum and their protective influence on Cr(VI) targeted to bovine serum albumin. *J. Agric. Food Chem.* **59**(14), 7902–7909 (2011)
26. Wang, C.-X., Ye, L., Yan, F.-F., Wang, N., Yu, P.-L.: Spectroscopic studies on the interaction between Rifabutin and human serum albumin. *Chem. J. Chin. Univer. Chin.* **28**(12), 2280–2283 (2007)
27. Liu, Y., Chen, M., Bian, G., Liu, J., Song, L.: Spectroscopic investigation of the interaction of the toxicant, 2-naphthylamine, with bovine serum albumin. *J. Biochem. Mol. Toxicol.* **25**(6), 362–368 (2011)
28. Zhao, X., Lu, D., Hao, F., Liu, R.: Exploring the diameter and surface dependent conformational changes in carbon nanotube-protein corona and the related cytotoxicity. *J. Hazard. Mater.* **292**, 98–107 (2015)
29. Chanphai, P., Tajmir-Riahi, H.: Tea polyphenols bind serum albumins: a potential application for polyphenol delivery. *Food Hydrocolloids* **89**, 461–467 (2019)
30. Chowdhury, R., Chattoraj, S., Sen Mojumdar, S., Bhattacharyya, K.: FRET between a donor and an acceptor covalently bound to human serum albumin in native and non-native states. *Phys. Chem. Chem. Phys.* **15**(38), 16286–16293 (2013)

Publisher's Note Springer Nature remains neutral with regard to jurisdictional claims in published maps and institutional affiliations.